Food & Function

ROYAL SOCIETY OF CHEMISTRY

PAPER

View Article Online
View Journal | View Issue

Cite this: *Food Funct.*, 2025, **16**, 4399

Exploring the lipid-lowering effects of cinnamic acid and cinnamaldehyde from the perspective of the gut microbiota and metabolites†

Xueke Wang, ‡[a,b] Tianxing Li,‡[b] Ling Dong,[c] Yilin Li,[b] Hong Ding,[d] Jing Wang,[d] Yuqi Xu,[d] Wenlong Sun *[c] and Lingru Li*[b]

The increasing incidence and associated metabolic complications pose major challenges in the treatment of hyperlipidaemia. Cinnamon is a food and medicinal resource associated with lipid metabolism, but the mechanism by which its active components, cinnamic acid (CA) and cinnamaldehyde (CM), alleviate hyperlipidaemia remains unclear. Biochemical, pathological, gut microbiota, and metabolomic analyses were performed to investigate the effects of CA and CM on HFD-fed mice and the underlying mechanisms involved. Supplementation with CA and CM reduced body weight, liver, and adipose tissue accumulation in HFD-induced mice; improved glucose and lipid metabolism; and decreased inflammation and oxidative stress levels, with CM showing superior efficacy. Faecal microbiota transplantation confirmed that the therapeutic effect was closely related to core gut bacteria and metabolites. Specifically, CA and CM inhibited the growth of lipid metabolism-related genera (*e.g.*, *Turicibacter* and *Romboutsia*) and metabolites (*e.g.*, PC, LysoPCs, prostaglandin E2, and arachidonic acid) while promoting the growth of beneficial genera (*e.g.*, *Oscillospiraceae* and *Colidextribacter*) and metabolites (*e.g.*, linoleic acid, phytosphingosine, and stercobilin). Additionally, Spearman's correlation analysis revealed that serum and hepatic lipids, as well as inflammatory factors, were positively correlated with *Erysipelatoclostridium*, *Turicibacter*, *Eubacterium fissicatena*, *Enterorhabdus*, cervonoyl ethanolamide, and acetoxystachybotrydial acetate, whereas they were negatively correlated with *Lachnospiraceae NK4A136*, stercobilin, LysoPE (15:0/0:0), and phytosphingosine. In contrast, hepatic oxidative stress markers exhibited the opposite correlation pattern. In conclusion, CA and CM have the potential to regulate the core gut microbiota and metabolites to improve lipid metabolism and decrease related inflammation and oxidative stress levels.

Received 20th January 2025,
Accepted 10th April 2025

DOI: 10.1039/d5fo00384a

rsc.li/food-function

Introduction

Hyperlipidaemia is characterized by lipid metabolism and lipoprotein disorders in the blood.[1] Elevated serum lipid levels can not only lead to atherosclerosis, increasing the risk of coronary heart disease, stroke, and peripheral arterial disease, but also potentially cause hypertension, acute pancreatitis, and fatty liver, which seriously threaten human health.[2] Currently, approximately 39% of adults worldwide have hyperlipidaemia. With the westernization of lifestyles and changes in dietary structure, the incidence of hyperlipidaemia is steadily increasing and tends to affect younger individuals.[3,4] Lifestyle adjustments, such as limiting the intake of high-fat and high-calorie foods, are the safest approach for controlling hyperlipidaemia. However, the adherence to long-term caloric restrictions is often poor, and relying solely on caloric limitation typically does not yield lipid-lowering effects. Therefore, many patients still require medication to reach their treatment goals.[5] Currently available medications, such as statins, bile acid sequestrants, and niacin, inhibit cholesterol synthesis or prevent the intestinal reabsorption of bile acids. However, the long-term use of these drugs is associated with adverse events, including myalgia, elevated liver enzymes, gastrointestinal discomfort, and constipation.[6] Additionally, owing to cost issues, long-term adherence to medication is also poor, which further hinders treatment effectiveness.[7,8] Therefore, increasing

[a]*Department of Encephalopathy, Henan Province Hospital of TCM (The Second Affiliated Hospital of Henan University of Chinese Medicine), Zhengzhou 450000, Henan, China*
[b]*National Institute of Traditional Chinese Medicine Constitution and Preventive Treatment of Diseases, Beijing University of Chinese Medicine, Beijing 100029, China*
[c]*Institute of Biomedical Research, Shandong University of Technology, Zibo, 255000 Shandong, China*
[d]*Second Clinical Medical School, Henan University of Chinese Medicine, Zhengzhou 450046, Henan, China*
†Electronic supplementary information (ESI) available. See DOI: https://doi.org/10.1039/d5fo00384a
‡These authors contributed equally to this article.

research has begun to focus on safe, effective and cost-effective lipid-lowering strategies, and natural functional products with biological activity will become potential research objects.

Recent studies have shown a strong correlation between the gut microbiota and hyperlipidaemia.[9,10] Specifically, the gut microbiota influences the lipid metabolism balance of the host through various mechanisms, including bile acid metabolism, the production of short-chain fatty acids (SCFAs), the inhibition of cholesterol absorption, and the regulation of inflammatory responses.[11] Dietary structure is a significant factor influencing the composition and metabolic pathways of the gut microbiome,[12] and long-term high-fat diets (HFDs) can lead to dysbiosis in the gut microbiota, resulting in an imbalance in the intestinal microbial ecosystem.[13] Conversely, functional foods or traditional Chinese herbal medicine can alleviate metabolic diseases by modulating the gut microbiota.[14] Fresh corn bracts reduce the proportion of Firmicutes and Bacteroidetes, promote the proliferation of bifidobacteria, and reduce the weight gain, insulin resistance, and oxidative damage caused by a HFD.[15] Wheat β-glucan can reduce the intestinal *Firmicutes*/*Bacteroidetes* ratio and decrease the abundance of *Coriobacteriaceae UCG-002*, *Romboutsia*, *Faecalibaculum* and *Enterorhabdus* in HFD-fed mice, thus playing an anti-hyperlipidaemic role.[16] Therefore, strategies for modulating the gut microbiome have been proposed as novel and effective treatments for limiting lipid accumulation in the body.

Cinnamon as a medicine and food is derived from the same source and is widely used in medicine and food as a spice and food additive. More than 80 compounds have been identified from different parts of cinnamon, among which cinnamic acid (CA) and cinnamaldehyde (CM) exhibit various biological functions, such as antibacterial, antioxidant, and anti-inflammatory activities and gut microbiota regulation.[17–19] In a randomized controlled trial involving 750 participants, cinnamon supplementation significantly reduced blood triglyceride and total cholesterol concentrations.[20] Animal experiments have shown that CA and CM can promote the browning of white adipose tissue in HFD-fed mice; reduce body weight, fat and lipid levels; and play a role in weight loss.[21,22] CA can effectively treat chronic constipation by improving the composition and abundance of the gut microbiota to regulate the production of SCFAs.[23] CM improves metabolic function in streptozotocin-induced diabetic mice by modulating the gut microbiota.[24] However, to our knowledge, it remains unclear whether CA and CM alleviate hyperlipidaemia through the gut microbiota and related mechanisms.

Therefore, the aim of this study was to investigate whether CA and CM can alleviate glucose and lipid metabolism disorders and decrease inflammatory responses and oxidative stress levels in HFD-induced hyperlipidaemic mice, as determined by observing changes in related indicators after treatment. Given the relationship between the gut microbiota and hyperlipidaemia, we employed 16S rRNA sequencing and untargeted metabolomics to explore the core gut bacteria and metabolites that CA and CM affect in alleviating HFD-induced hyperlipidaemia in mice. Our findings provide new insights into the potential mechanisms by which CA and CM mitigate hyperlipidaemia through the regulation of the gut microbiota and metabolites.

Materials and methods

Chemicals and reagents

Simvastatin (SV, B21384), cinnamic acid (CA, B21082) and cinnamaldehyde (CM, B21081) with purities greater than 95% were purchased from Shanghai Yuanye Biotechnology Co., Ltd (Shanghai, China). Methyl cellulose (MC, 0.1%, M8070) was purchased from Solarbio (Beijing, China) and used to dissolve SV, CA and CM. The control diet (D10012G, containing 15.8% fat, 20.3% protein, and 63.9% carbohydrates, 3.9 kcal g^{-1}) and high-fat diet (D12109C, containing 40% fat, 20% protein, and 40% carbohydrates, 4.5 kcal g^{-1}) were both provided by Changzhou Biotechnology Co., Ltd (Jiangsu, China) (Table S1†). Neomycin sulfate, metronidazole, ampicillin, and vancomycin were purchased from Macklin (Shanghai, China).

Animal experimental design

Six-week-old C57BL/6 mice weighing 18–20 grams were purchased from Beijing Vital River Laboratory Animal Technology Co., Ltd (licence no. SCXK 2021-0006, Beijing, China) and housed at the Laboratory Animal Center of the Beijing University of Chinese Medicine (SPF grade). All the mice were maintained in a standard environment at room temperature and relative humidity with a 12-hour light/dark cycle. Our study was conducted in accordance with international ethical guidelines and was approved by the Laboratory Animal and Ethics Committee of Beijing University of Chinese Medicine (ethics no. 2024-004-M).

After 1 week of adaptive feeding, mice were randomly divided into 5 groups to apply different feed and gavage approaches: NC group (standard diet and gavage of the same volume of 0.1% MC), HC group (HFD and gavage of the same volume of 0.1% MC), SV group (HFD and daily gavage of 30 mg kg^{-1} SV), CA group (HFD and daily gavage of 20 mg kg^{-1} CA), and CM group (HFD and daily gavage of 20 mg kg^{-1} CM). During the 12-week intervention, the mice were gavaged daily, weight was recorded weekly, and food intake and water intake were recorded daily.

The pseudo germ-free (PGF) model was established by combining penicillin G (600 mg kg^{-1} d^{-1}), metronidazole (600 mg kg^{-1} d^{-1}), neomycin sulfate (600 mg kg^{-1} d^{-1}) and vancomycin (180 mg kg^{-1} d^{-1}) for 1 week. The mice were randomly assigned by weight. Faecal samples from donor mice in the HC, CA and CM groups were collected in sterile test tubes, diluted with sterile normal saline (0.2 g mL^{-1}), and filtered with sterile gauze to remove particles before inoculation. The FHC, FCA and FCM groups were established by the intragastric administration of faecal bacteria from the HC, CA and CM groups to PGF mice for 14 days. The HFD was continued after faecal bacteria transplantation until the 10th week or death. In

the faecal bacteria transplantation experiment, the mice were intragastrically administered bacteria daily, weight was recorded weekly, and food intake and water intake were recorded daily.

Sample collection

Before the experiment ended, fresh faeces were collected from the mice housed in metabolic cages. At the end of the experiment, the mice in each group were fasted for 12 hours and weighed, and then anaesthetized with isoflurane. Blood was collected *via* the orbital venous plexus, followed by centrifugation (1600 rpm for 10 minutes at 4 °C) to obtain the serum. The mice were euthanized by cervical dislocation. The liver and adipose tissues (epididymal fat, inguinal fat, and brown adipose tissue) were isolated, weighed, and collected. All the samples were stored at −80 °C for subsequent analysis.

Biochemical index detection

Serum total cholesterol (TC), triglyceride (TG), low-density lipoprotein cholesterol (LDL-C), high-density lipoprotein cholesterol (HDL-C), alanine aminotransferase (ALT), aspartate aminotransferase (AST), and faecal total cholesterol (TC) and triglyceride (TG) levels were measured using commercial kits (Jiancheng Bioengineering Institute, Nanjing, China). Lipopolysaccharide (LPS), interleukin-6 (IL-6), interleukin-1 beta (IL-1β), and tumour necrosis factor-alpha (TNF-α) were measured using ELISA kits (Cusabio, Wuhan, China). Liver tissue samples were pretreated by mixing the tissue with a homogenization reagent at a weight-to-volume ratio of 1 : 9, followed by homogenization on ice to form a 10% homogenate. The homogenate was then centrifuged (2500 rpm, 10 minutes), and the supernatant was retained. Total protein in the tissue homogenate was measured using a BCA protein assay kit. The levels of total cholesterol (TC), triglyceride (TG), alanine transaminase (ALT), and aspartate transaminase (AST) in the liver were measured using commercial kits (Jiancheng Bioengineering Institute, Nanjing, China). The activities of catalase (CAT), total superoxide dismutase (T-SOD), glutathione peroxidase (GSH-Px), and malondialdehyde (MDA) and the level of reduced glutathione (GSH) in the liver were measured using commercial kits (Jiancheng Bioengineering Institute, Nanjing, China).

Hematoxylin/eosin (H&E) staining

Mouse livers were fixed in 4% paraformaldehyde, and epididymal white adipose tissue, inguinal white adipose tissue, and brown adipose tissue were fixed with a fat-specific fixative. Following the manufacturer's instructions, the liver and adipose tissue samples were embedded in paraffin and sectioned into 3 μm slices. The sections were stained using an H&E staining kit (Solarbio, Beijing, China).

16S rRNA gene sequencing

The gut microbiota of each group of mice (n = 8) was analysed using 16S rDNA high-throughput sequencing. Fresh faecal pellets were collected directly from the anus of each mouse into sterile sampling tubes, quickly flash-frozen in liquid nitrogen, and stored at −80 °C as soon as possible. The genomic DNA of the gut microbiota was extracted from the faecal samples using an EZNA® soil DNA kit according to the manufacturer's instructions and electrophoresed through a 1% agarose gel. A NanoDrop2000 was utilized to assess DNA quality. PCR amplification of the V3–V4 hypervariable region of the 16S rRNA gene was subsequently performed using FastPfu polymerase and dedicated primer sets. The PCR cycling conditions were as follows: an initial denaturation step at 95 °C for 3 minutes, followed by 27 cycles of denaturation at 95 °C for 30 seconds, annealing at 55 °C for 30 seconds, and extension at 72 °C for 45 seconds. The reaction was terminated with a final extension step at 72 °C for 10 minutes. The upstream primer used was 338F (5′-ACTCCTACGGGAGGCAGCAG-3′), and the downstream primer used was 806R (5′-GGACTACHVGGGTWTCTAAT-3′). The reaction for each sample was replicated three times to ensure reproducibility. The PCR products generated from each identical sample were combined, and the pooled PCR amplicons were subsequently purified utilizing a commercially available purification kit. The purified PCR products were cleaned using an AxyPrep DNA gel extraction kit and visualized *via* 2% agarose gel electrophoresis. The precise concentration and quantity of the PCR products were subsequently determined using a Quantus™ fluorometer (Promega, USA). The Illumina MiSeq PE300/NovaSeq PE250 platform was utilized for sequencing to generate high-quality sequencing data. The sequences were subjected to quality filtering to ensure reliability and accuracy. The operational taxonomic units (OTUs) were subsequently clustered on the basis of a sequence similarity threshold of 97% and a confidence level of 70%. The community composition of each sample was then analysed and characterized at various taxonomic levels.

Fecal metabolomic analysis

Faecal samples were accurately weighed for LC-MS/MS analysis, and 400 μL of a methanol/water (4 : 1, v/v) mixture was added to extract metabolites. After extraction, the supernatant was centrifuged at 13 000g at 4 °C for 15 minutes and then transferred to vials for subsequent analysis. Additionally, 20 μL of the supernatant from each sample was pooled to prepare a quality control sample. The instrument platform used for LC-MS analysis was the AB SCIEX UHPLC-triple TOF system. The specific analytical methods and parameter settings are provided in ESI Table 2.† Using the R package "ropls" (version 1.6.2), orthogonal least partial squares discriminant analysis (OPLS-DA) was conducted alongside 7-cycle interactive validation to assess model stability. Differentially abundant metabolites between the two groups were mapped to their respective biochemical pathways *via* metabolic enrichment and pathway analyses using the KEGG database (**https://www.genome.jp/kegg/**). The Python package "scipy.stats" (**https://docs.scipy.org/doc/scipy/**) was used to conduct enrichment analysis, with the aim of identifying the most pertinent biological pathways associated with the experimental treatments.

Correlations between the colonic microbiota and the screened metabolites were investigated using Spearman's correlation analysis.

Statistical analysis

All data are shown as the mean ± SEM, and data processing was performed using GraphPad Prism 8. Differences among experimental groups were statistically analysed by one-way ANOVA with Tukey's *post hoc* test. A difference was deemed statistically significant when $p < 0.05$. The presence of distinct alphabetical markers indicates that there are significant differences between two groups.

Results

Effects of CA and CM on the serum lipid profile, blood glucose, and inflammatory factors in HFD-fed mice

Body weight and organ weight are direct indicators of lipid accumulation in mice. There were no significant differences in initial body weight among the groups ($p > 0.05$). After 12 weeks of continuous feeding, the body weights of the mice in all the groups increased to varying degrees. At the end of 12 weeks, compared with those in the NC group, the body weights of the mice in the HC group significantly increased ($p < 0.05$), whereas the final body weights of the mice in the SV, CA and CM groups significantly decreased after supplementation ($p < 0.05$). There was no significant difference in body weight between the SV and CA groups ($p > 0.05$), and there was no significant difference between the CM and NC groups ($p > 0.05$) (Fig. 1B and C). Owing to the greater energy density of the HFD, mice fed a HFD had greater energy intake, despite no significant difference in food intake. Interestingly, SV, CA and CM significantly reduced the body and tissue (liver, epididymal, and inguinal adipose tissue) weight gain induced by the HFD without affecting water intake, food intake, or energy intake ($p < 0.05$, Fig. S1A–G†), suggesting that supplementation with SV, CA and CM may promote fat expenditure rather than suppress appetite. Serum and faecal lipid measurements from each group revealed that after 12 weeks of HFD feeding, the serum levels of TC, TG, and LDL-C were elevated, whereas HDL-C levels were decreased. Supplementation with SV, CA and CM significantly reduced the serum TC, TG, and LDL-C levels ($p < 0.05$), with little effect on HDL-C ($p > 0.05$). Compared with that in the SV group, the decrease in the serum TC level was less pronounced ($p < 0.05$), while there was no significant difference in the serum TG level ($p > 0.05$). Among the drug intervention groups, there was no significant difference in LDL-C between the SV and CA groups ($p > 0.05$), whereas the CM group presented the greatest decrease ($p < 0.05$) (Fig. 1D–G). Additionally, higher lipid (TC and TG) levels were measured in the faeces of the HC, SV, CA, and CM

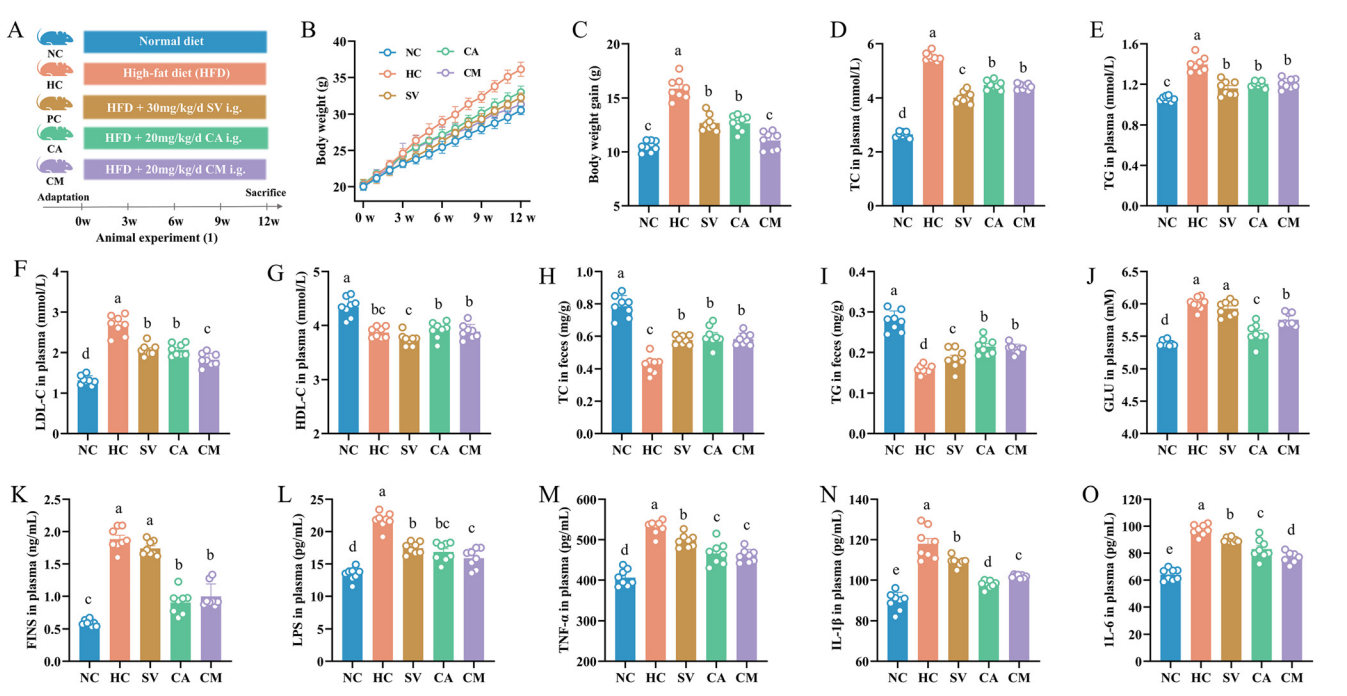

Fig. 1 Effects of CA and CM on the serum lipid profile and the levels of blood glucose and inflammatory factors in HFD-fed mice. (A) Experimental grouping and protocol for CA and CM interventions. (B) Body weight changes over 12 weeks. (C) Body weight gain in HFD-fed mice. (D) TC, (E) TG, (F) LDL-C, and (G) HDL-C levels in plasma; (H) TC and (I) TG levels in faeces; and (J) GLU, (K) FINS, (L) LPS, (M) TNF-α, (N) IL-1β, and (O) IL-6 levels in plasma. The data are presented as means of biological replicates ± SEMs ($n = 8$). Differences between groups were analysed using one-way ANOVA followed by Tukey's *post hoc* test. Statistical significance was set at $p < 0.05$. Different letters indicate significant differences between groups. HFD, high-fat diet; NC, normal control group; HC, hyperlipidaemic group; SV, simvastatin control group (HFD and 30 mg kg^{-1} SV); CA, cinnamic acid group (HFD and 20 mg kg^{-1} CA); CM, cinnamaldehyde group (HFD and 20 mg kg^{-1} CM); ANOVA, analysis of variance.

groups, indicating that more lipids were excreted in the intestine than absorbed ($p < 0.05$, Fig. 1H and I). Long-term HFD feeding caused abnormal glucose and insulin metabolism, while supplementation with CA and CM significantly reduced the serum GLU and FINS levels ($p < 0.05$). Compared with the HC group, the SV group presented no significant effects on GLU or FINS (Fig. 1J and K).

Long-term HFD consumption leads to chronic low-grade inflammation in the body, promoting the release of inflammatory factors. Continuous HFD feeding for 12 weeks resulted in significant increases in the serum levels of LPS, TNF-α, IL-6, and IL-1β ($p < 0.05$). However, supplementation with SV, CA and CM significantly alleviated this trend ($p < 0.05$, Fig. 1L–O). Compared with those in the SV group, the serum TC levels in the CA and CM groups were not significantly lower ($p < 0.05$), while there was no significant difference in the serum TG levels ($p > 0.05$). Among the drug intervention groups, there was no significant difference in LDL-C between the SV and CA groups ($p > 0.05$), whereas the CM group presented the greatest decrease ($p < 0.05$). These results suggest that CA and CM have positive effects on glucose and lipid metabolism as well as inflammatory factor levels in HFD-fed mice.

Effects of CA and CM on hepatic oxidative stress, lipid levels, and histopathology in HFD-fed mice

Chronic HFD feeding increases oxidative stress levels, leading to an accumulation of lipid peroxides and subsequent liver cell damage. Compared with the NC group, the HC group exhibited significant decreases in liver SOD, CAT, and GSH-Px activity and GSH levels ($p < 0.05$), whereas MDA levels significantly increased ($p < 0.05$). However, supplementation with SV, CA and CM resulted in significant increases in liver SOD, CAT, and GSH-PX activities and GSH levels, along with significant decreases in MDA levels ($p < 0.05$). Compared with those in the SV group, the activities of SOD, CAT and GSH-PX in the liver and the GSH level were greater in the CA and CM groups, and the MDA level was lower ($p < 0.05$); however, there was no significant difference between the CA and CM groups ($p > 0.05$, Fig. 2A–E). A long-term chronic high-fat diet can lead to excessive lipid accumulation in the liver, resulting in fatty liver, which in turn affects liver function and may cause hepatocyte damage and inflammation. After 12 weeks of high-fat feeding, the liver lipids in the mice significantly accumulated (TC and TG) ($p < 0.05$). However, after supplementation with SV, CA and CM, the liver TC and TG levels significantly decreased ($p < 0.05$). Compared with that in the SV group, there was no significant difference in liver TC in the CA group. However, liver TC was greater in the CM group ($p < 0.05$), and liver TG was also greater in both the CA and CM groups ($p < 0.05$, Fig. 2F and G). ALT and AST are important indicators for evaluating liver function damage. Compared with the NC group, the HC group presented severe liver function impairment, which was reversed by supplementation with SV, CA and CM ($p < 0.05$, Fig. S1H–K†). Hepatocyte swelling and fatty degeneration are common pathological changes caused by long-term HFD feeding. After 12 weeks of HFD feeding, H&E staining of liver tissue from the mice revealed hepatocyte swelling, enlarged lipid droplets, and a significant increase in fat content. However, after supplementation with SV, CA and CM, the swelling of hepatocytes was alleviated, the number of lipid droplets was reduced, and the fat content significantly decreased ($p < 0.05$, Fig. 2H and I). These results suggest that CA and CM can significantly reduce liver lipid accumulation induced by a long-term HFD, resolve liver function damage, and alleviate hepatocyte swelling and fatty degeneration.

H&E staining of adipose tissue more intuitively reveals changes in adipocyte structure, the extent of fat accumulation, and histopathological changes in tissue, thus helping to uncover the histological basis of metabolic abnormalities. As shown in Fig. 2J–L, adipocytes in the HC group were significantly enlarged. Lipid droplets in brown adipose tissue cells were enlarged and tended to transform into white adipose tissue, with a weakening of the typical characteristics of brown adipose tissue.

After supplementation with SV, CA and CM, the adipocyte volume decreased, lipid droplet accumulation decreased, and the trend of brown adipose tissue conversion into white adipose tissue was reversed. In summary, these results indicate that CA and CM can alleviate liver oxidative stress and reduce lipid levels induced by a HFD, reduce adipose tissue accumulation, and potentially have a protective effect on the liver.

FMT confirms the role of the gut microbiota in the mechanisms by which CA and CM alleviate hyperlipidaemia

To elucidate the role of the gut microbiota in the therapeutic effects of CA and CM, faecal microbiota transplantation (FMT) was applied to HFD-fed mice. The experimental protocol is shown in Fig. 3A. Compared with those of the FHC group, the FMT of CA- and CM-treated mice significantly reduced weight gain and organ weights (Fig. 3B and C and Fig. S2D–G†), but there were no significant differences in food intake, caloric intake, or water consumption ($p > 0.05$, Fig. S2A–C†). Similarly, compared with those in the FHC group, the serum lipid, blood glucose, and inflammatory marker levels were significantly lower in the FCA and FCM groups ($p < 0.05$, Fig. 3D–M). Furthermore, with respect to liver lipids, liver function, and liver H&E staining results, mice in the FCA and FCM groups presented significant decreases in liver lipids (TC and TG) ($p < 0.05$, Fig. 3N and O) and improvements in liver function ($p < 0.05$, Fig. S2H–K†), alleviated hepatocyte swelling, reduced lipid droplet size, and a significant decrease in fat content ($p < 0.05$, Fig. 3P and Q). H&E staining of adipose tissue revealed that FCA and FCM mice had smaller eWAT and iWAT adipocytes, reduced lipid droplet accumulation, and a slowing trend of brown adipose tissue conversion into white adipose tissue (Fig. S2L–N†). In conclusion, the recipient mice presented phenotypes and trends similar to those of the donor mice, suggesting that the efficacy of CA and CM is closely related to the gut microbiota.

Effects of CA and CM on the gut microbiota of HFD-fed mice

To investigate the effects of CA and CM on the gut microbiota in HFD-fed mice, we collected faecal samples and performed

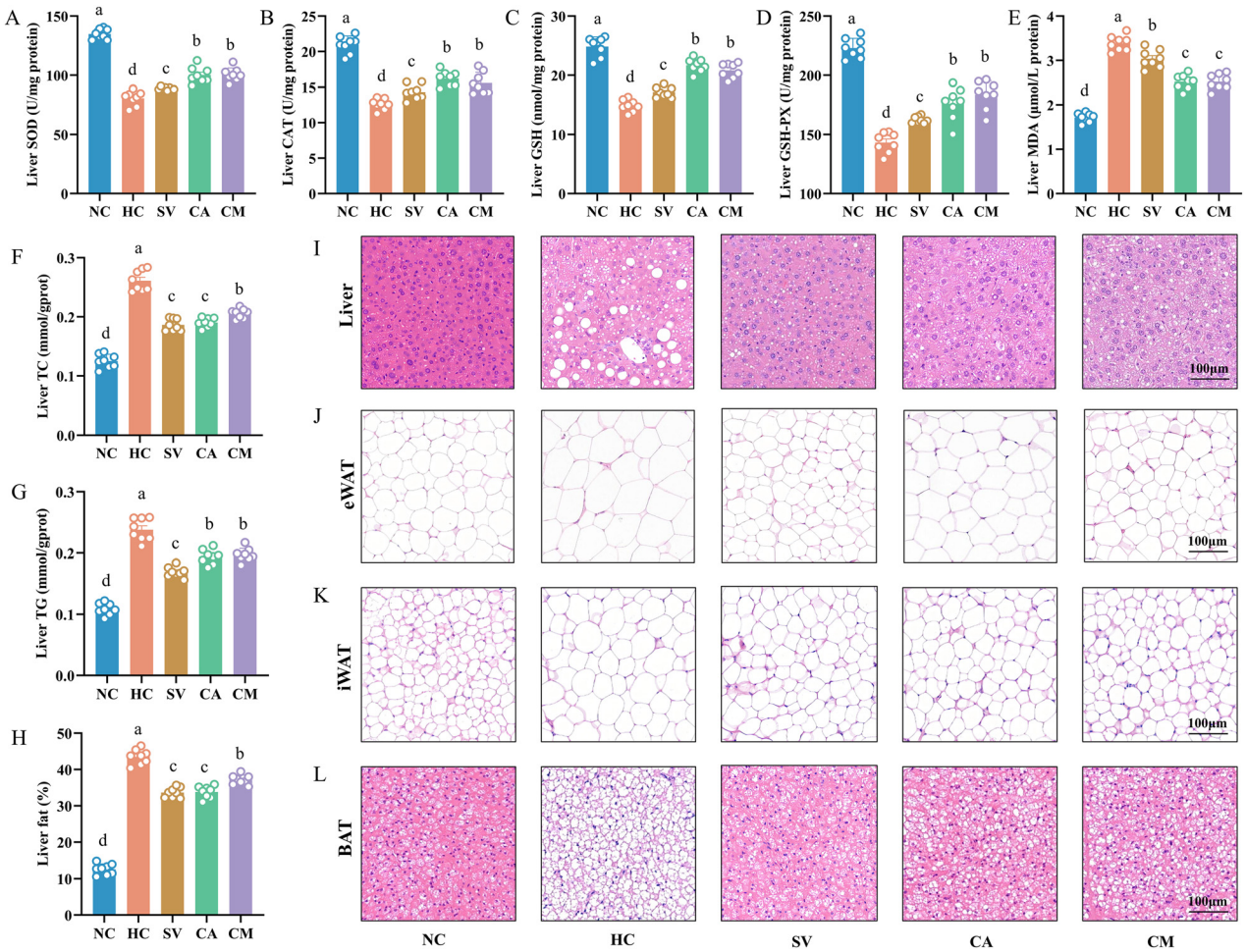

Fig. 2 Effects of CA and CM on hepatic oxidative stress, lipid levels, and histopathology in HFD-fed mice. (A) SOD, (B) CAT, (C) GSH, (D) GSH-PX, (E) MDA, (F) TC, and (G) TG levels in liver homogenates. (H) Liver fat ratio. H&E staining of (I) liver tissue, (J) epididymal white adipose tissue (eWAT), (K) inguinal white adipose tissue (iWAT), and (L) brown adipose tissue (BAT) from mice. Scale bar, 100 μm. The data are presented as means of biological replicates ± SEMs (n = 8). Differences between groups were analysed using one-way ANOVA followed by Tukey's *post hoc* test. Statistical significance was set at $p < 0.05$. Different letters indicate significant differences between groups. HFD, high-fat diet; NC, normal control group; HC, hyperlipidaemic group; SV, simvastatin control group (HFD and 30 mg kg^{-1} SV); CA, cinnamic acid group (HFD and 20 mg kg^{-1} CA); CM, cinnamaldehyde group (HFD and 20 mg kg^{-1} CM); ANOVA, analysis of variance.

16S rRNA V3–V4 analysis. Compared with the CON group, the HFD group presented decreases in the Sobs (Fig. 4A), Ace (Fig. 4B), Chao1 (Fig. S3A†), and Shannon (Fig. S3B†) indices, whereas supplementation with CA and CM partially restored the diversity and richness of the gut microbiota. These results were consistent with the Venn diagram, which revealed an increase in the number of OTUs after supplementation with CA and CM (Fig. S3C†). Beta diversity analysis *via* principal coordinate analysis (PCoA) (Fig. 4C) and nonmetric multidimensional scaling analysis (NMDS) (Fig. S3D†) indicated that supplementation with CA and CM significantly altered the gut microbiota structure in HFD-fed mice. Analysis of the Bray–Curtis distance revealed that BSP supplementation reshaped the overall structure of the gut microbiota, making it more similar to that of the NC group (Fig. S3E†). Next, we analysed the effects of CA and CM on the composition of the gut microbiota at the phylum (Fig. 4D) and genus (Fig. S3F†) levels.

The gut microbiota was predominantly composed of *Firmicutes* (approximately 70%), followed by *Bacteroidetes* and *Desulfobacterota*. The HFD increased the abundance of *Firmicutes* and *Actinobacteria*, while reducing the abundance of *Bacteroidetes*. The ratio of *Firmicutes* to *Bacteroidetes* (F/B) is an important indicator reflecting the composition and homeostasis of the intestinal microbiota and is closely related to the metabolic status of the host. Compared with that in the NC group, the F/B ratio in the HC group was significantly greater ($p < 0.05$), and supplementation with CA and CM significantly reduced the F/B ratio ($p < 0.05$, Fig. 4E). A cluster heatmap (Fig. 4F) showed that the abundances of *Turicibacter*, *Romboutsia*, *Eubacterium fissicatena*, and *Enterorhabdus* in the guts of the mice increased after HFD feeding, whereas the

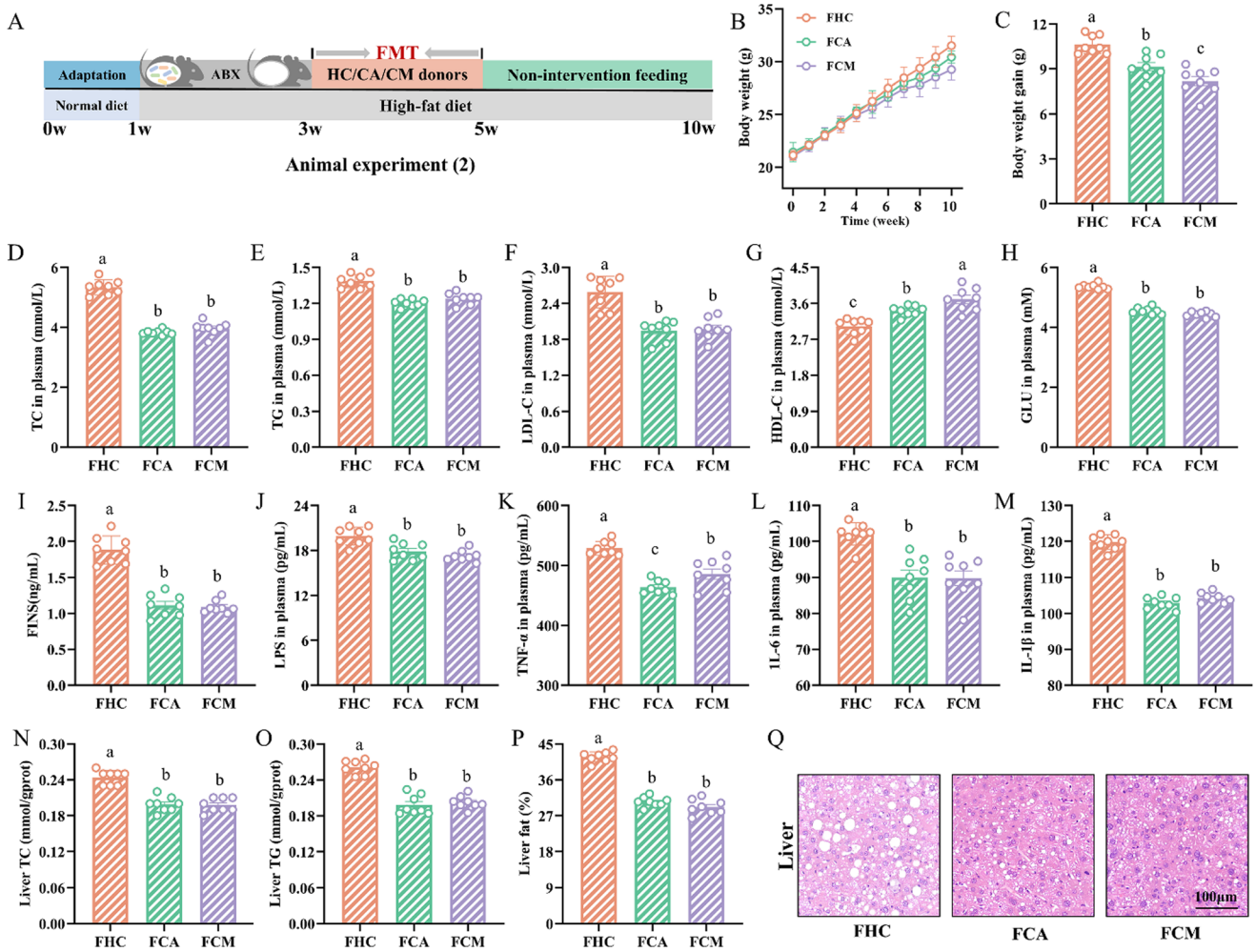

Fig. 3 FMT confirms the role of the gut microbiota in the mechanisms by which CA and CM alleviate hyperlipidaemia. (A) Experimental grouping and protocol for FMT. (B) Body weight changes over 12 weeks. (C) Body weight gain. (D) TC, (E) TG, (F) LDL-C, (G) HDL-C, (H) GLU, (I) FINS, (J) LPS, (K) TNF-α, (L) IL-6, and (M) IL-1β levels in plasma. (N) TC and (O) TG levels in the liver. (P) Liver fat ratio. (Q) Representative H&E staining of liver tissue from mice. Scale bar, 100 μm. The data are presented as means ± SEMs from biological replicates (n = 8). Differences between the experimental groups were analysed using one-way ANOVA followed by Tukey's *post hoc* test. Differences were considered statistically significant when $p < 0.05$. Different letters indicate significant differences between two groups. HFD, high-fat diet; FHC, faecal microbiota transplantation of the HC group; FCA, faecal microbiota transplantation of the CA group; FCM, faecal microbiota transplantation of the CM group; ANOVA, analysis of variance.

abundances of these microbiota decreased after supplementation with CA and CM. Moreover, CA and CM supplementation increased the relative abundances of *Roseburia*, *Oscillospiraceae*, and *Colidextribacter*.

Furthermore, clustering analysis revealed that the CA and CM groups, particularly the CA group, clustered closely with the NC group, suggesting that CA and CM reshaped the gut microbiota, making it more similar to the microbiota of mice fed a standard diet. To explore the specific gut microbiota regulated by CA and CM, we generated a taxonomic cladogram (Fig. 4G) and histogram (Fig. S3G†) of the LDA score on the basis of LEfSe analysis, which revealed taxonomic groups with LDA scores greater than 4. At the genus level, the differential genus in the NC group was *Dubosiella*, whereas the differential genera in the HFD group included *Romboutsia*, *Eubacterium fissicatena*, *Turicibacter*, and *Enterorhabdus*. The characteristic genera of the CA group were *Ruminococcus torques*, *Colidextribacter*, and *Marvinbryantia*, whereas the characteristic genera of the CM group were *Blautia* and *Lachnospiraceae NK4A136*.

Additionally, according to linear regression analysis, liver TC (Fig. 4H) and liver TG (Fig. 4I) were significantly correlated with the observed Sobs index and accounted for 64.5% and 62.29% of the variation in the Sobs index, respectively (Fig. 4H and I). We also performed correlation analysis *via* the Spearman algorithm to explore the relationships between gut bacterial genera and biochemical markers in mice after supplementation with CA or CM. As shown in Fig. S3H,† *Enterorhabdus*, *Eubacterium fissicatena*, *Romboutsia*, and *Turicibacter* were positively correlated with TC, TG, IL-6, IL-1β, TNF-α, and LPS and negatively correlated with SOD, GSH, CAT, and GSH-PX. *Akkermansia*, *Oscillospiraceae*, and *Colidextribacter*

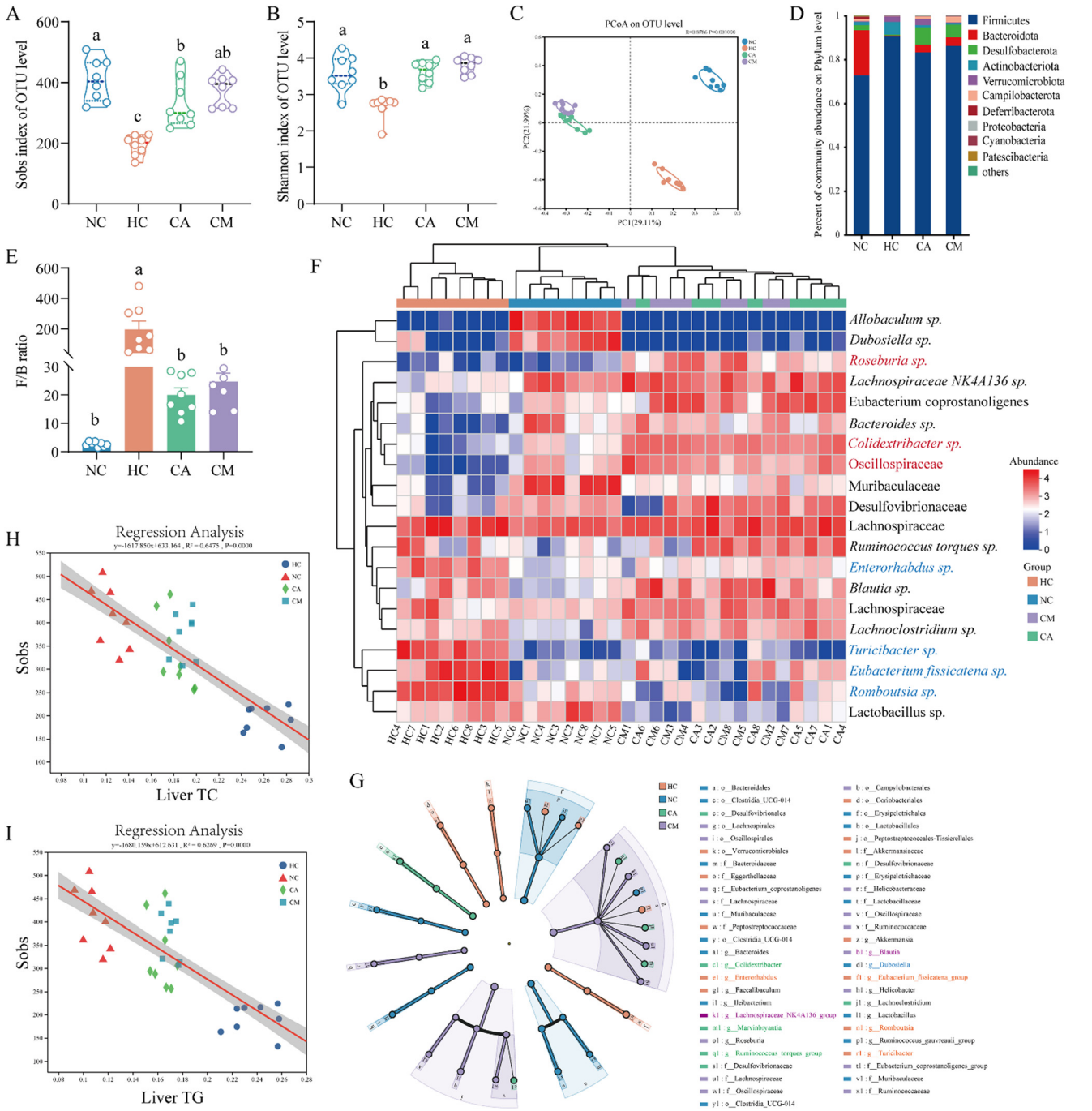

Fig. 4 Effects of CA and CM on the gut microbiota of HFD-fed mice. (A) The Sob index at the OTU level. (B) The Shannon index at the OTU level. (C) PCoA of the gut microbiota. (D) The composition profile of the gut microbiota assessed at the phylum level. (E) F/B ratio. (F) Heatmap of the relative abundance of the top 20 genera at the OTU level. (G) Taxonomic cladogram of the LDA score based on LEfSe analysis (LDA > 4 was considered the differential characteristic taxon). Regression analysis (H) between liver TC and the Sobs index and (I) between liver TG and the Sobs index. The data are presented as means of biological replicates ± SEMs (n = 8). Differences between groups were analysed using one-way ANOVA followed by Tukey's *post hoc* test. Statistical significance was set at $p < 0.05$. Different letters indicate significant differences between groups. NC, normal control group; HC, hyperlipidaemic group; CA, cinnamic acid group (HFD and 20 mg kg^{-1} CA); CM, cinnamaldehyde group (HFD and 20 mg kg^{-1} CM); ANOVA, analysis of variance.

were negatively correlated with TC, TG, IL-6, IL-1β, TNF-α, and LPS and positively correlated with SOD, GSH, CAT, and GSH-PX. In summary, these microorganisms, such as *Romboutsia*, *Eubacterium fissicatena*, *Oscillospiraceae*, and *Colidextribacter*, can be considered potential biomarkers for regulating the gut microbiota to prevent and improve lipid metabolism.

Effects of CA and CM on the gut metabolite profiles of HFD-fed mice

The gut microbiota plays an important role in the metabolism of exogenous substances, leading to the production of and variation in certain small-molecule metabolites. Therefore, we conducted an untargeted metabolomic study to identify the effects of CA and CM supplementation on the metabolic profiles of HFD-fed mice. After the raw data were processed, 2251 and 2557 mass spectrometry peaks were extracted in positive and negative ion modes, respectively, for all the samples. The RSD of the QC samples was <0.3, and the cumulative proportion of peaks was >70%, indicating that the analytical method for metabolomics in this study was stable and reproducible (Fig. S4A†). The Venn diagram of metabolites revealed the similarities and differences in metabolites produced between the groups, with the overlapping portions indicating common metabolic differences among the groups (Fig. S4B†). The PLS-DA results demonstrated that, in both positive and negative ion modes, there was clear separation and 27 and 57 decreased metabolites, respectively. After comparison with the database (VIP > 2, FC > 2, and $p < 0.05$), 48, 38, and 46 differentially abundant metabolites were identified between the NC and HC groups, CA and HC groups, and CM and HC groups, respectively (Tables S3–S5†). PLS-DA model validation revealed that the $R2$ values in both positive and negative ion modes were above Q2, with the intercepts of the Q2 regression lines on the Y-axis being −0.6165 and −0.5675, indicating that the model had a good fit and strong predictability, making it suitable for subsequent data analysis (Fig. S4C and D†).

The clustering heatmap (Fig. 5F) and bar charts of differentially abundant metabolites (Fig. S4E–M†) indicated that CA and CM inhibited the increase in Pc (14:0/P-18:1(11*Z*)), Pc (18:0/0:0), Pc (22:0/16:0), Lysopc (15:0), Lysopc (P-18:1(9*Z*)/0:0), Lysopc (17:0/0:0), Lysopc (0:0/16:0), Lysopc (20:1(11*Z*)/0:0), leukotriene C4 (LTC4), prostaglandin E2 (PGE2), and arachidonic acid (AA) induced by the HFD and inhibited the decrease in linoleic acid, phytosphingosine, stercobilin, and Pgp (20:4 (5*Z*,8*Z*,11*Z*,14*Z*)/22:6(4*Z*,7*Z*,10*Z*,13*Z*,16*Z*,19*Z*)) caused by the HFD. We then performed pathway enrichment analysis (impact value >0.4, $P < 0.05$), which revealed that the HFD significantly affected 5 pathways (Fig. 5G). Both CA and CM regulated the linoleic acid metabolism, alpha-linolenic acid metabolism, glycerophospholipid metabolism, and arachidonic acid metabolism pathways. Additionally, CA and CM influenced sphingolipid metabolism and the biosynthesis of unsaturated fatty acids, respectively (Fig. 5H and I). A linkage diagram between metabolic pathways and changes in related metabolites is shown in Fig. 6, suggesting that CA and CM may restore the normal function of metabolic pathways by regulating changes in metabolites, thereby suppressing the occurrence and development of hyperlipidaemia.

Additionally, correlation analysis between the intestinal core flora and metabolites (Fig. 5J) and the biochemical indices and intestinal metabolites (Fig. S4N†) revealed that Lysopc (20:1(11*Z*)/0:0), arachidonic acid metabolism, Lysopc (15:0), Pc (14:0/P-18:1(11*Z*)), Lysopc (0:0/16:0), Lysopc (17:0/0:0), and Pc (22:0/16:0) were positively correlated with *Romboutsia*, *Eubacterium fissicatena*, serum and liver lipids (TC and TG) and serum inflammatory markers (IL-1β, LPS, IL-6, and TNF-α) and negatively correlated with *Colidextribacter* and *Oscillospiraceae* and liver oxidative stress indicators (GSH, GSH-PX, SOD, and CAT). Linoleic acid, Pgp (20:4 (5*Z*,8*Z*,11*Z*,14*Z*)/22:6(4*Z*,7*Z*,10*Z*,13*Z*,16*Z*,19*Z*)), LC4, PE2, and stercobilin were negatively correlated with *Romboutsia*, *Eubacterium fissicatena*, serum and liver lipids (TC and TG) and serum inflammatory markers (IL-1β, LPS, IL-6 and TNF-α) and positively correlated with *Colidextribacter* and *Oscillospiraceae* and liver oxidative stress markers (GSH, GSH-PX, SOD, and CAT).

Correlation analysis of biochemical indicators related to hyperlipidaemia, the gut microbiota, and metabolites

To elucidate the significance of CA and CM in alleviating hyperlipidaemia through the modulation of the gut microbiota and metabolites, we conducted Spearman's correlation analysis to explore the relationships among hyperlipidaemia-related biochemical markers, the gut microbiota, and metabolites. The correlation network diagrams demonstrated significant correlations ($|R| > 0.6$, $p < 0.05$) among biochemical markers (lipids and inflammatory and oxidative stress markers), microbiota, and metabolites (Fig. 7). Overall, serum and liver lipids (TC and TG) were positively correlated with *Erysipelatoclostridium*, *Lachnospiraceae*, *Turicibacter*, *Eubacterium fissicatena*, *Enterorhabdus*, linoleic acid, cervonoyl ethanol, 12-hydroxyoctadecanoic acid, and acetoxystachybotrydial acetate and negatively correlated with *Lachnospiraceae NK4A136*, stercobilin, Lysope (15:0/0:0:0), and phytosphingosine. LPS, TNF-α, and IL-6 were positively correlated with *Erysipelatoclostridium*, *Turicibacter*, *Eubacterium fissicatena*, *Enterorhabdus*, cervonoyl ethanolamide, and acetoxystachybotrydial acetate and negatively correlated with *Lachnospiraceae NK4A136*, stercobilin, Lysope (15:0/0:0), and phytosphingosine. Liver CAT, GSH, GSH-PX, and SOD were positively correlated with *Lachnospiraceae NK4A136*, stercobilin, phytosphingosine, arachidonic acid, and Icosa-2,4,6-trienoic acid and negatively correlated with *Erysipelatoclostridium*, *Turicibacter*, *Enterorhabdus*, cervonoyl ethanolamide, and acetoxystachybotrydial acetate. These results suggest that the aforementioned genera and metabolites can be considered biomarkers for hyperlipidaemia. In conclusion, CA and CM may alleviate hyperlipidaemia by modulating the gut microbiota and metabolic pathways.

Discussion

Hyperlipidaemia, a global public health issue, is a risk factor for various chronic diseases.[3] Cinnamon holds promise as a feasible alternative for the prevention and alleviation of obesity and lipid metabolism disorders.[25] However, the potential of its main active components, CA and CM, in preventing

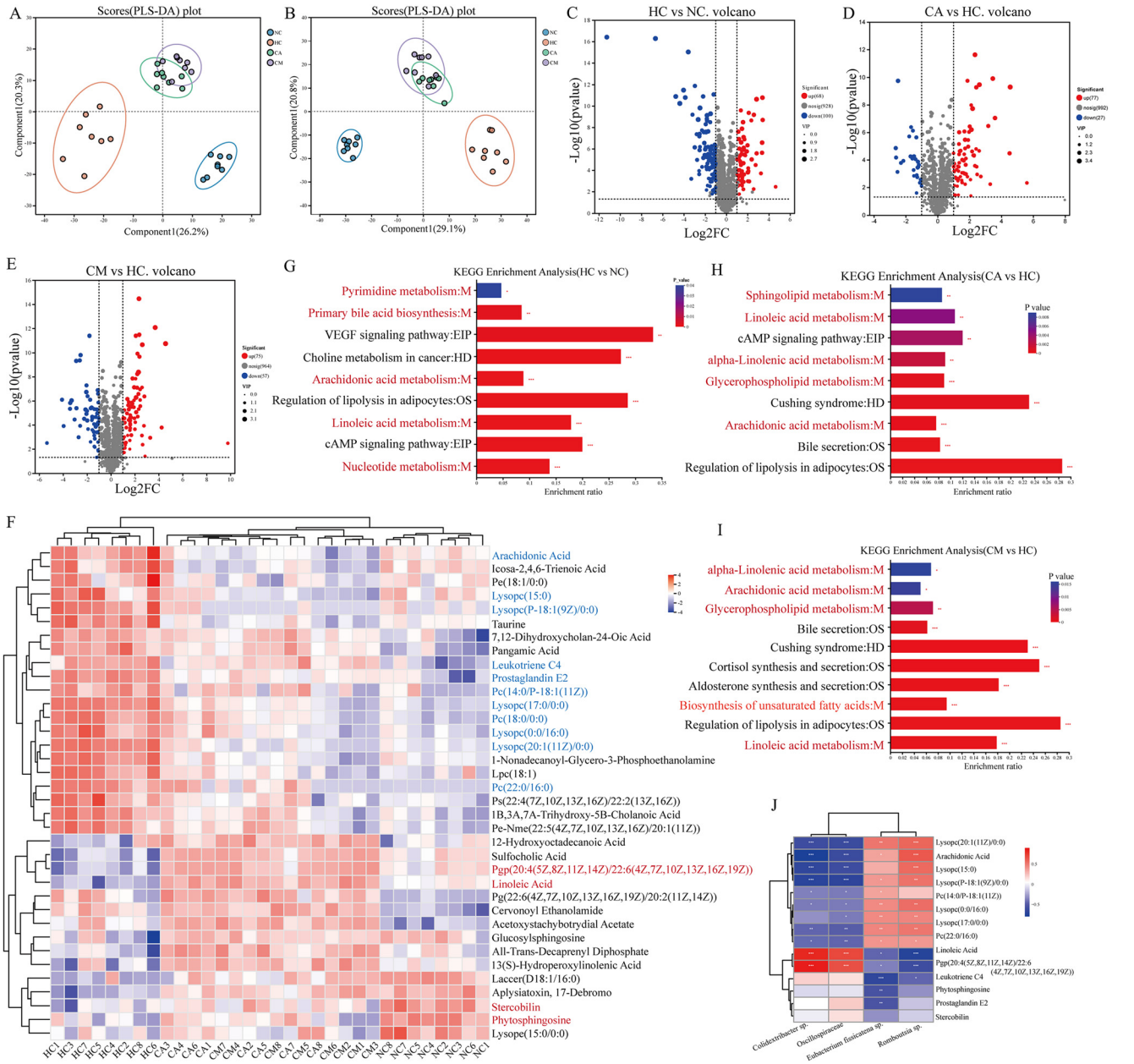

Fig. 5 Effects of CA and CM on the gut metabolite profiles of HFD-fed mice. PLS-DA in (A) positive mode and (B) negative mode comparing the NC, HC, CA and CM groups. Volcano plot depicting the differentially abundant metabolites (C) between the HC and NC groups, (D) between the CA and HC groups, and (E) between the CM and HC groups. (F) Heatmap of all the differentially abundant metabolites. Metabolic pathway enrichment analysis (G) between the HC and NC groups, (H) between the CA and HC groups, and (I) between the CM and HC groups in positive and negative ionization modes. (J) Spearman's correlation analysis between the metabolites and the core microbiota. The data are presented as means of biological replicates ± SEMs (n = 8). Differences between groups were analysed using one-way ANOVA followed by Tukey's *post hoc* test. Statistical significance was set at $p < 0.05$. Different letters indicate significant differences between groups. NC, normal control group; HC, hyperlipidaemic group; CA, cinnamic acid group (HFD and 20 mg kg^{-1} CA); CM, cinnamaldehyde group (HFD and 20 mg kg^{-1} CM); ANOVA, analysis of variance.

and treating hyperlipidaemia remains unclear. In this study, we evaluated the effects of CA and CM on the phenotypes, gut microbiota, and metabolites of hyperlipidaemic mice, as well as potential associations. The findings may provide an effective approach for functional food interventions targeting hyperlipidaemia. In this study, mice were fed a control diet (15.8% of calories from fat) or a high-fat diet (HFD, 40% of calories from fat) supplemented with CA or CM to investigate the causal relationships among CA, CM, the gut microbiota, and hyperlipidaemia. The results demonstrated that the daily gavage of 20 mg kg^{-1} CA and CM has significant potential in alleviating HFD-induced hyperlipidaemia in mice. These effects included reduced body weight, improved glucose and lipid metabolism, alleviated inflammation, enhanced anti-

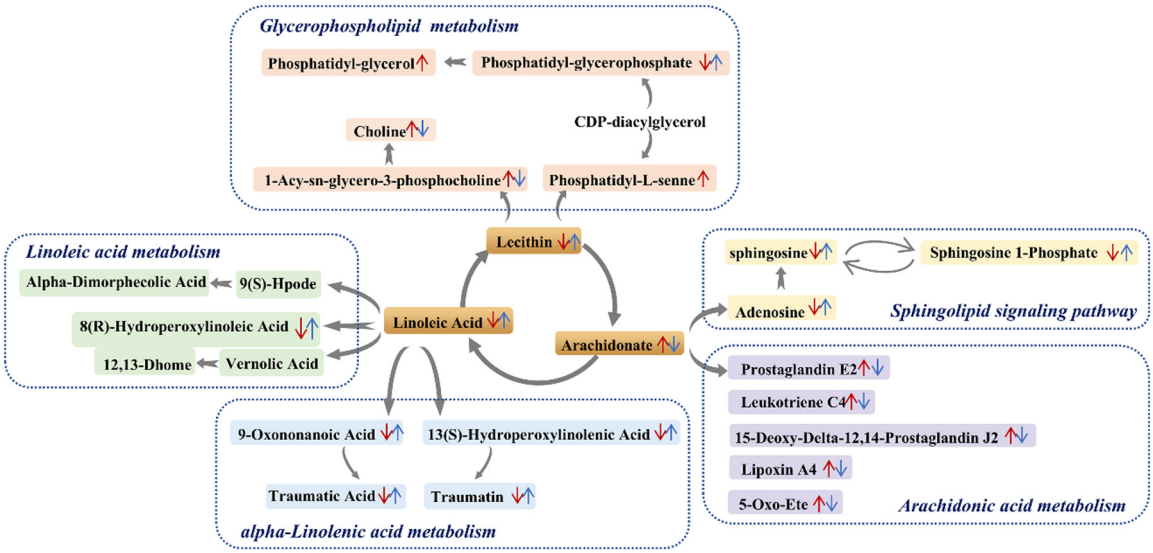

Fig. 6 Metabolic network based on differentially abundant metabolites and pathway analysis. The red and blue arrows represent metabolites regulated by a HFD and CA/CM, respectively.

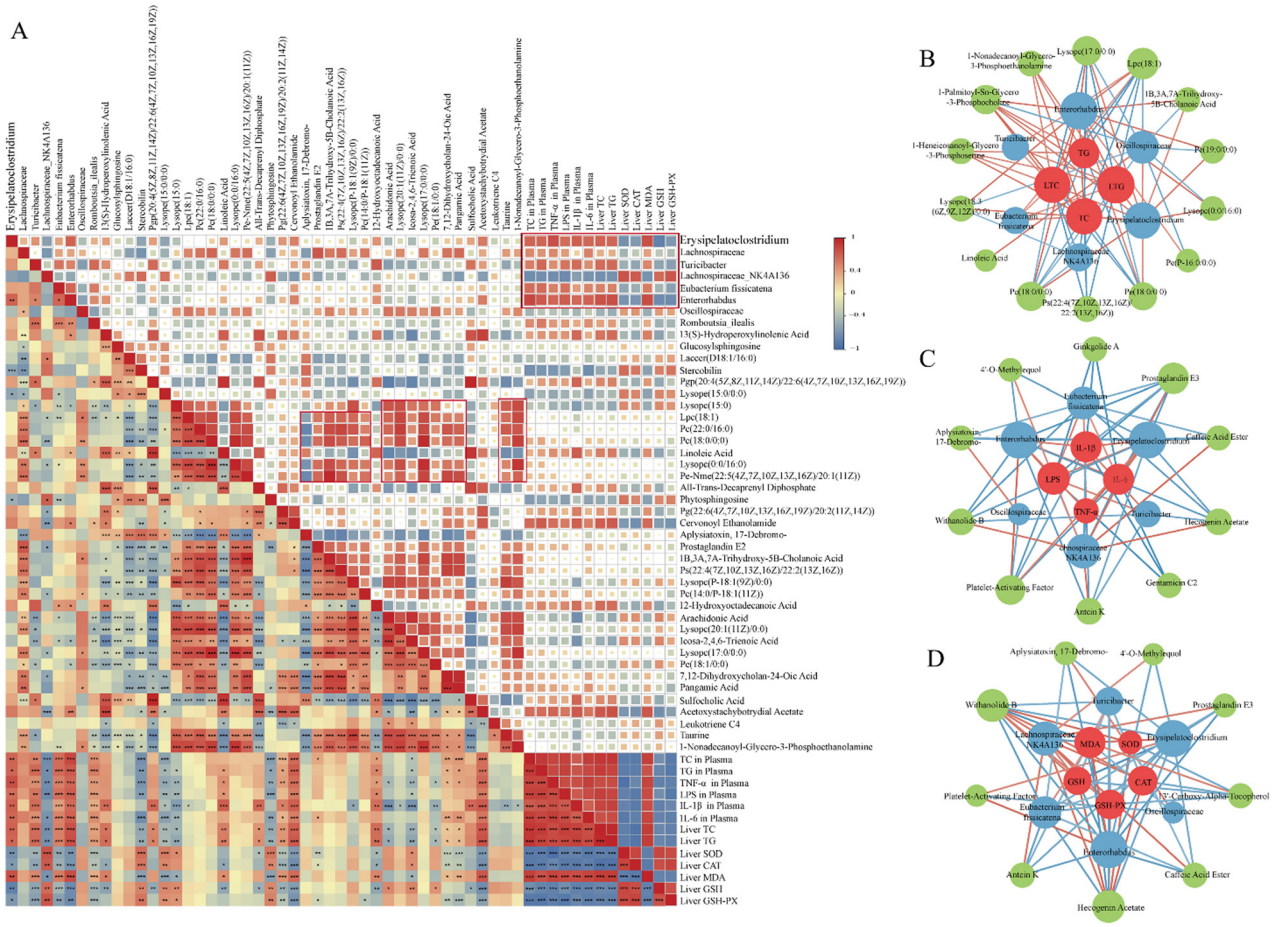

Fig. 7 Spearman's correlation (A) heatmap and network among (B) serum and liver lipids, (C) the serum inflammatory index, and (D) the hepatic oxidative stress index, the gut microbiota, and differentially abundant metabolites. Red nodes represent biochemical indicators, blue nodes represent the gut microbiota, and green nodes represent differentially abundant metabolites. The red lines indicate positive correlations, whereas the blue lines indicate negative correlations.

oxidant capacity, and modulation of the gut microbiota and metabolites (experiment 1). Furthermore, faecal microbiota transplantation experiments confirmed that the therapeutic effects of CA and CM may be mediated through their regulation of the gut microbiota and metabolites (experiment 2).

Studies have shown that CA can improve weight gain and serum lipid distribution in HFD-fed rats and that CA derivatives have antioxidant and lipid-lowering effects on hyperlipidaemic rats.[26] CM can decrease serum lipid, oxidative stress, and inflammatory factor levels in HFD-fed rats, exerting an anti-atherosclerotic effect.[27] In this study, we found that supplementation with CA and CM reduced the levels of total TC, TG, and LDL-C in serum, while HDL-C levels did not significantly increase. Among them, the improvement of serum TG levels by CA and CM was similar to that of SV, while CM showed a better effect on LDL-C improvement compared to SV. After supplementation with CA and CM, the serum GLU, FINS, LPS, and inflammatory cytokine (TNF-α, IL-6, and IL-1β) levels significantly decreased. These effects were superior to those of supplementation with SV. The decrease in these biochemical indicators was closely related to the reversal of gut microbiota dysbiosis by CA and CM, affecting the core gut microbiota and metabolites. For example, the F/B ratio was reduced, and the growth of lipid metabolism-related genera (such as *Enterorhabdus*, *Turicibacter*, and *Romboutsia*) was inhibited, whereas the growth of beneficial bacteria (such as *Roseburia*, *Oscillospiraceae*, and *Colidextribacter*) was promoted.

Research has shown that gut microbiota dysbiosis, including abnormalities in composition, structure, and function, is closely associated with various chronic metabolic diseases, such as obesity, diabetes, and cardiovascular diseases.[28] Promoting or inhibiting the growth of specific microorganisms is an effective way to influence the host phenotype. *Roseburia* can stimulate the differentiation of Treg cells through the production of butyrate, alleviating inflammation, enhancing the intestinal barrier, and reducing the risk of obesity; it is also negatively correlated with BMI, blood glucose, and blood lipids.[29] *Oscillospiraceae* is involved in the synthesis of butyrate and other SCFAs, which typically help maintain gut homeostasis and host health. A prospective study has shown that *Oscillospira* is negatively correlated with body weight, blood lipids, and inflammation.[30] *Colidextribacter* is a beneficial anti-inflammatory bacterium.[31] Studies have shown that *Colidextribacter* has a positive effect on mice with nonalcoholic fatty liver disease (NAFLD) induced by a HFD.[32] In this study, supplementation with CA and CM promoted the growth of *Roseburia*, *Oscillospiraceae*, and *Colidextribacter*, which were negatively correlated with lipids (TC and TG) and inflammatory factors (IL-6, IL-1β, TNF-α, and LPS) and positively correlated with oxidative stress markers (SOD, GSH, CAT, and GSH-PX). Notably, the characteristic genera of the HFD group were *Enterorhabdus*, *Turicibacter*, *Eubacterium fissicatena* and *Romboutsia*, which are generally considered harmful bacteria. The increase in *Enterorhabdus* may be associated with glucose and lipid metabolism, as well as fat accumulation, suggesting that *Enterorhabdus* may promote the occurrence of metabolic abnormalities.[33] An increased abundance of *Turicibacter* can exacerbate intestinal damage and lead to severe complications.[34] *Eubacterium fissicatena* and *Romboutsia* are considered potential pathogens in the gut and are associated with colonic inflammation and oxidative stress levels.[35] *Ruminococcus torques*, *Colidextribacter*, and *Marvinbryantia* were characteristic differential genera in the CA group, whereas *Blautia* and *Lachnospiraceae NK4A136* were characteristic differential genera in the CM group and generally considered beneficial bacteria. Among them, *Marvinbryantia* has a relatively high abundance in healthy populations and is negatively correlated with liver cirrhosis.[36] *Blautia* has the ability to biotransform compounds, regulate host health, and alleviate metabolic syndrome.[37] *Lachnospiraceae NK4A136* positively impacts the host's overall metabolic health by promoting gut barrier function, regulating glucose and lipid metabolism, and alleviating inflammation.[38] Notably, in the present study, supplementation with CA and CM reduced the increase in the abundance of harmful bacteria such as *Turicibacter*, *Romboutsia*, *Eubacterium fissicatena*, and *Enterorhabdus* compared with those in the HC group, but increased the relative abundance of beneficial bacteria such as *Roseburia*, *Oscillospiraceae*, and *Colidextribacter*. These results suggest that supplementation with CA and CM is associated with promoting or inhibiting the growth of beneficial or harmful bacteria related to lipid metabolism, which may explain how CA and CM reshape the gut microbiota to alleviate hyperlipidaemia. However, further research is needed to confirm the roles of these genera in the development of hyperlipidaemia.

The metabolic products of the gut microbiota, such as lipopolysaccharides (LPS), SCFAs, and secondary bile acids, are important regulatory factors for host physiological functions. These metabolites can enter the bloodstream through the permeability of the intestinal barrier, affecting the metabolic functions of various tissues and organs and reflecting the host health status.[39] Through pathway analysis, this study identified five lipid metabolism pathways affected by a HFD, among which CA and CM regulate linoleic acid metabolism, glycerophospholipid metabolism, arachidonic acid metabolism, alpha-linolenic acid metabolism, and sphingolipid metabolism. Studies have shown that CA and CM inhibited the increase in Lysopc (15:0), Lysopc (P-18:1(9*Z*)/0:0), Lysopc (17:0/0:0), Lysopc (0:0/16:0), Lysopc (20:1(11*Z*)/0:0), Pc (14:0/P-18:1(11*Z*)), Pc (18:0/0:0), and Pc (22:0/16:0) induced by a HFD. These metabolites were positively correlated with blood lipids (TC and TG) and inflammatory factors (IL-6, IL-1β, TNF-α, and LPS) and negatively correlated with oxidative stress markers (GSH, GSH-PX, CAT, and SOD). Supplementation with CA and CM reversed the decreases in linoleic acid, Pgp (20:4(5*Z*,8*Z*,11*Z*,14*Z*)/22:6(4*Z*,7*Z*,10*Z*,13*Z*,16*Z*,19*Z*)), phytosphingosine, and stercobilin, which were positively correlated with blood lipids (TC and TG) and inflammatory factors (IL-6, IL-1β, TNF-α, and LPS) and negatively correlated with oxidative stress markers (GSH, GSH-PX, CAT, and SOD).

Phosphatidylcholine (PC) plays important roles in lipid metabolism, cell signalling, and gut health.[40] Zhang *et al.* reported that, compared with those in a blank group (ND), the

levels of 10 PC species in ApoE$^{-/-}$ mice fed a HFD were significantly greater than those in the ND group, a finding that is consistent with the results of our research.[41] LysoPCs are minor components of the cell membrane, and are formed by the hydrolysis of PC, and have the ability to regulate LDL-C metabolism. They are involved in atherosclerosis induced by sterols and may also damage endothelial cells by inducing lipid peroxidation of the cell membrane.[42,43] According to the research by Yu *et al.*, a HFD increases lipid profiles such as PC, LysoPCs, and fatty acids; in particular, they suggested that LysoPCs could be considered potential biomarkers for chronic HFD intake in nonobese individuals.[44] Linoleic acid is known to promote lipid metabolism and alleviate inflammation, which is beneficial for chronic diseases such as obesity and hyperlipidaemia.[45] P-glycoprotein (Pgp), an important membrane transporter, plays a key role in various physiological and pathological processes. Studies have shown that in Pgp-deficient mice fed a high-fat diet, body weight, fat mass, serum insulin, and glucose levels are greater, and metabolic disorders develop earlier.[46]

This result was consistent with our findings, where Pc (14:0/P-18:1(11*Z*)), Pc (22:0/16:0), linoleic acid, Lysopc (17:0/0:0), and Pgp (20:4(5*Z*,8*Z*,11*Z*,14*Z*)/22:6(4*Z*,7*Z*,10*Z*,13*Z*,16*Z*,19*Z*)) were negatively correlated with TC, TG, *Erysipelatoclostridium*, *Enterorhabdus*, *Romboutsia ilealis*, *Turicibacter*, and *Eubacterium fissicatena* and positively correlated with potentially beneficial bacteria such as *Lachnospiraceae* and *Oscillospiraceae*. These findings suggest that CA and CM may regulate linoleic acid, alpha-linolenic acid, and glycerophospholipid metabolism by increasing beneficial gut microbiota and reducing harmful bacteria, thereby decreasing lipid synthesis; this could also be one of the reasons for the reduction in serum and liver total cholesterol levels.

This study revealed that a HFD induced an increase in AA, PGE2, and LTC4 in the intestines of mice. CA and CM reversed this trend. Arachidonic acid is considered an important driver of the inflammatory response and is associated with the occurrence and development of many metabolic diseases, such as obesity, fatty liver disease and hyperlipidaemia.[47,48] In addition, a HFD can significantly promote the formation of oxidative derivatives of arachidonic acid (proinflammatory molecules such as prostaglandins, thromboxins and leukotrienes), which aggravate oxidative stress and the inflammatory response.[49] PE2, by binding to specific prostaglandin receptors, activates downstream signalling pathways that promote the release of inflammatory factors (such as IL-6 and TNF-α), increase vascular permeability, and exacerbate inflammation.[50] Similarly, LTC4 also increases vascular permeability, promoting the leakage of plasma proteins and white blood cells to the site of inflammation, thereby worsening the local inflammatory response.[51] This finding is consistent with the results of our study, which revealed that AA, PGE2, and LTC4 were positively correlated with IL-6, IL-1β, TNF-α, LPS, *Erysipelatoclostridium*, *Enterorhabdus*, *Romboutsia ilealis*, *Turicibacter*, and *Eubacterium fissicatena*. These findings suggest that these genera may accelerate the synthesis of AA, PGE2, and LTC4, promoting inflammation in the body, whereas CA and CM may alleviate the inflammatory response in hyperlipidaemic mice by reducing the abundance of these genera and metabolites.

There is interplay among lipid metabolism, inflammation, and oxidative stress. The dysregulation of lipid metabolism, especially the oxidation of fatty acids, promotes the generation of reactive oxygen species (ROS), which triggers oxidative stress. Oxidative stress further damages lipid components of cell membranes, leading to lipid peroxidation and the formation of harmful substances such as oxidized lipids. These substances not only disrupt cellular structures but also activate inflammatory pathways, promoting the release of pro-inflammatory cytokines such as IL-6 and TNF-α. Moreover, inflammation itself can exacerbate oxidative stress by increasing ROS levels within cells, creating a vicious cycle. This process is a key pathological mechanism in various metabolic diseases, such as obesity, hyperlipidaemia, and diabetes, induced by HFDs.[52] Obtusastyrene is an effective antimicrobial agent with anti-inflammatory and antioxidant properties.[53] Linoleic acid can activate transcription factors such as PPARs and SREBP, regulating fatty acid synthesis and oxidation processes, influencing fat storage and energy metabolism, and thereby impacting obesity.[54] This study revealed that liver SOD, GSH-PX, CAT, and GSH levels were negatively correlated with AA, PGE2, and LTC4 levels and positively correlated with linoleic acid, Lysopc (17:0/0:0), Pc (14:0/P-18:1(11*Z*)), and Pc (22:0/16:0) levels. These results suggest that CA and CM may regulate lipid metabolism and inflammatory responses by modulating the gut microbiota and metabolites, thereby alleviating oxidative stress and delaying the onset and progression of hyperlipidaemia.

This study employed a comprehensive approach, including analyses of blood lipid levels, blood glucose, inflammatory factors, and oxidative stress; histopathology; 16S rDNA sequencing; and metabolomics, to elucidate the therapeutic effects of CA and CM on hyperlipidaemia. The results showed that CA and CM effectively alleviated body weight and organ weight increases induced by a HFD in mice and reduced hyperlipidaemia-related dyslipidaemia, inflammation, oxidative stress, and liver damage. Additionally, through FMT, we confirmed that the therapeutic effects of CA and CM were largely mediated by the modulation of the gut microbiota and metabolites. Notably, supplementation with CA and CM reversed gut dysbiosis, lowered the F/B ratio, and primarily affected specific bacteria (*Romboutsia*, *Eubacterium fissicatena*, *Oscillospiraceae*, and *Colidextribacter*) and related metabolites (linoleic acid, PCs, Lysopcs, and AA), thereby alleviating hyperlipidaemia (Fig. 8). In conclusion, this study provides theoretical support for the potential of CA and CM as functional foods to improve lipid metabolism. In addition, we conducted a preliminary investigation of the relationships between biochemical markers, the gut microbiota, and metabolites using Spearman's correlation analysis, aiming to identify potential associations or common trends in their changes, which may provide clues for subsequent mechanistic studies. However, correlation analysis only reveals the associations between

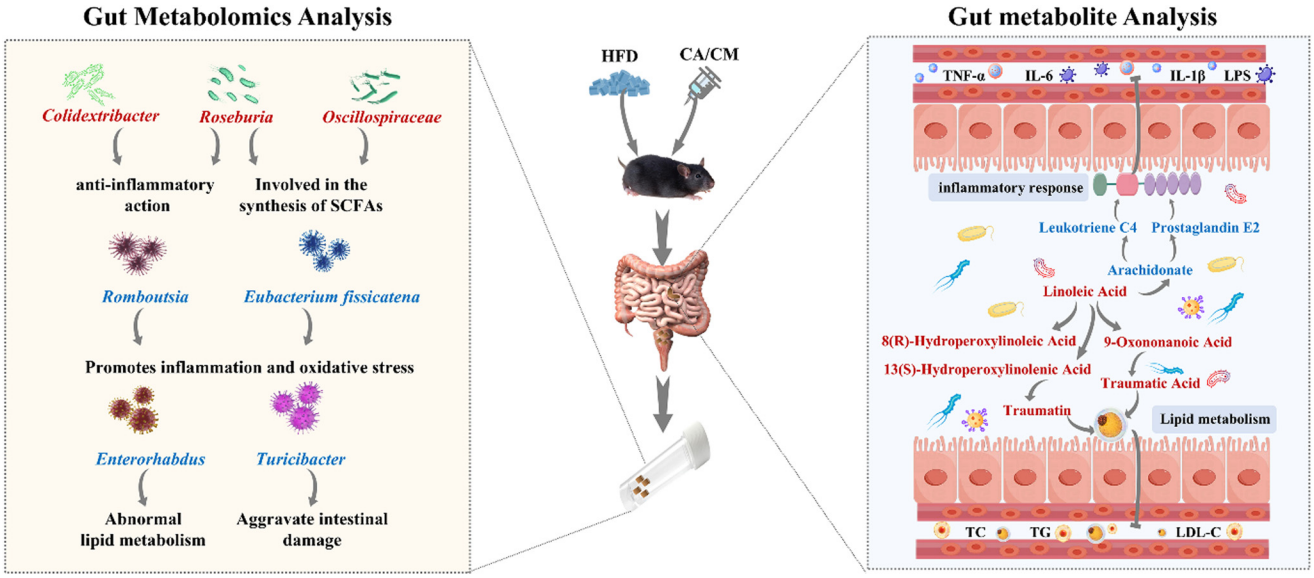

Fig. 8 Possible mechanism by which CA and CM alleviate hyperlipidaemia in mice by regulating the gut microbiota genera and metabolites.

these variables and cannot directly prove causal relationships or the direct impact of one feature on the changes in another. Therefore, further research is needed to gain a deeper understanding of how these factors interact and collectively influence physiological processes.

Conclusion

This study employed a comprehensive approach, including analyses of blood lipid levels, blood glucose, inflammatory factors, and oxidative stress; histopathology; 16S rDNA sequencing; and metabolomics, to elucidate the efficacy of CA and CM in hyperlipidaemia. The results indicate that CA and CM effectively reduce body weight and organ weight in HFD-fed mice, mitigating blood lipid abnormalities, inflammation, oxidative stress, and liver damage associated with hyperlipidaemia. Furthermore, we confirmed through FMT that the therapeutic effects of CA and CM are largely mediated by the regulation of the gut microbiota and metabolites. Notably, supplementation with CA and CM reversed gut microbiota dysbiosis and reduced the F/B ratio, which may activate lipid metabolism-related pathways to alleviate hyperlipidaemia. In conclusion, this study provides theoretical support for the improvement of glucose and lipid metabolism and inflammatory factors in hyperlipidaemic mice by CA and CM. However, the specific associations between the beneficial effects of CA and CM and the intestinal microbiota they regulate as well as the metabolites of these microbiota still need to be further studied and confirmed.

Author contributions

Xueke Wang and Tianxing Li: conceptualization, methodology, data curation, and writing – original draft. Ling Dong and Yilin Li: resources. Hong Ding: validation. Jing Wang and Yuqi Xu: supervision. Wenlong Sun: supervision and writing – review & editing. Lingru Li: supervision, project administration and funding acquisition.

Data availability

All data for this study are provided in this article and its ESI.† The raw data presented in the main text and ESI† will be made available upon request from the first author or the corresponding author. The related microbiome data have been organized and are available for download at **https://www.ncbi.nlm.nih.gov/bioproject/1242482**.

Conflicts of interest

The authors have no conflicts of interest to declare.

Acknowledgements

This work was supported by the National Natural Science Foundation of China (no. 82374308), the National Key Research and Development Program of China (no. 2022YFC2010104), the Key Research and Development Program of Shandong (no. 2021SFGC1205), the High Level Key Discipline of National Administration of Traditional Chinese Medicine – Traditional Chinese Constitutional Medicine (no. zyyzdxk-2023251), the Henan Province Key Research and Development and Promotion Special Project (Science and Technology Tackling Project) (no. 242102311066 and 252102311014), and the Doctoral Research Fund Project of Henan Provincial Hospital of Traditional Chinese Medicine (no. 2024BSJJ12).

References

1 A. J. Berberich and R. A. Hegele, A Modern Approach to Dyslipidemia, *Endocr. Rev.*, 2022, **43**, 611–653.
2 J. Ballard-Hernandez and J. Sall, Dyslipidemia Update, *Nurs. Clin. North Am.*, 2023, **58**, 295–308.
3 H. Yanai, H. Adachi, M. Hakoshima, M. Hakoshima and H. Katsuyama, Postprandial Hyperlipidemia: Its Pathophysiology, Diagnosis, Atherogenesis, and Treatments, *Int. J. Mol. Sci.*, 2023, **24**, 13942.
4 Q. Zhang, D. Zhang, X. Zhou, Q. Li, N. He, J. Zhang, Q. Gu and Z. Qian, Antihyperlipidemic and Hepatoprotective Properties of Vitamin B6 Supplementation in Rats with High-Fat Diet-Induced Hyperlipidemia, *Endocr., Metab. Immune Disord.: Drug Targets*, 2021, **21**, 2260–2272.
5 M. Arvanitis and C. J. Lowenstein, Dyslipidemia, *Ann. Intern. Med.*, 2023, **176**, ITC81–ITC96.
6 C. A. Aguilar-Salinas, R. A. Gómez-Díaz and P. Corral, New Therapies for Primary Hyperlipidemia, *J. Clin. Endocrinol. Metab.*, 2022, **107**, 1216–1224.
7 M. Ruscica, N. Ferri, M. Banach, C. R. Sirtori and A. Corsini, Side effects of statins: from pathophysiology and epidemiology to diagnostic and therapeutic implications, *Cardiovasc. Res.*, 2023, **118**, 3288–3304.
8 B. D. Pino and F. Sbrana, Therapeutic adherence in hyperlipidemia: When one size doesn't fit all, *Eur. J. Intern. Med.*, 2023, **112**, 143–145.
9 J. Zhang, Y. Zhang, G. Yang, W. Zhang, K. Thakur, Z. Nib and Z. Wei, Carboxymethylated Lycium barbarum seed dreg dietary fiber alleviates high fat diet-induced hyperlipidemia in mice via intestinal regulation, *Food Funct.*, 2024, **15**, 6955–6965.
10 L. Chen, Y. Lei, C. Lu, D. Liu, W. Ma, H. Lu and Y. Wang, Punicic acid ameliorates obesity-related hyperlipidemia and fatty liver in mice via regulation of intestinal flora and lipopolysaccharide-related signaling pathways, *Food Funct.*, 2024, **15**, 5012–5025.
11 L. Cao, Y Wu, K. Liu, N. Qi, J. Zhang, S. Tie, X. Li, P. Tian and S. Gu, *Cornus officinalis* vinegar alters the gut microbiota, regulating lipid droplet changes in nonalcoholic fatty liver disease model mice, *Food & Medicine Homology*, 2024, **1**, 9420002.
12 Y. Liu, C. Liu, Y. Deng, Y. Chen, Q. Qiu, X. Shang, C. Wang, L. Han, L. Huang, Z. Yang, L. Xiao, X. Fang and X. Li, Beneficial effects of dietary herbs on high-fat diet-induced obesity linking with modulation of gut microbiota, *Food & Medicine Homology*, 2025, **2**, 9420034.
13 L. Han, C. Hu, Z. Du, H. Yu, Y. Du, L. Li, F. Li, Y. Wang, X. Gao, X. Sun, Z. Zhang and Y. Qin, Association of glycerolipid metabolism with gut microbiota disturbances in a hamster model of high-fat diet-induced hyperlipidemia, *Front. Cell. Infect. Microbiol.*, 2024, **14**, 1439744.
14 Y. Liu, N. Ling, B. Zhang, C. Chen, X. Mo, J. Cai, X. Tan and Q. Yu, Flavonoid-Rich mulberry leaf extract modulate lipid metabolism, antioxidant capacity, and gut microbiota in high-fat diet-induced obesity: potential roles of FGF21 and SOCS2, *Food & Medicine Homology*, 2024, **1**, 9420016.
15 N. Geng, Y. Li, Y. Zhang, H. Wang, J. Song, L. Yu and C. Wu, Effects of Modified Dietary Fiber from Fresh Corn Bracts on Obesity and Intestinal Microbiota in High-Fat-Diet Mice, *Molecules*, 2023, **28**, 4949.
16 M. Li, Q. Wang, X. Zhang, K. Li, M. Niu and S. Zhao, Wheat β-glucan reduces obesity and hyperlipidemia in mice with high-fat and high-salt diet by regulating intestinal flora, *Int. J. Biol. Macromol.*, 2024, **288**, 138754.
17 P. Ouyang, S. Huang, W. Wei, J. Wu, Y. Zhou, S. Li, Q. Li, Y. Geng, X. Huang, D. Chen and L. Yin, Cinnamaldehyde treats largemouth bass non-lethal bacterial enteritis by regulating gut morphology, barrier, inflammation, microbiota and serum biochemistry, *Int. J. Biol. Macromol.*, 2024, 581.
18 Y. Xiao, F. Zhang, H. Xu, C. Yang, X. Song, Y. Zhou, X. Zhou, X. Liu and J. Miao, Cinnamaldehyde microcapsules enhance bioavailability and regulate intestinal flora in mice, *Food Chem.: X*, 2022, **15**, 100441.
19 J. F. Malheiro, J. Maillard, F. Borges and M. Simões, Biocide Potentiation Using Cinnamic Phytochemicals and Derivatives, *Molecules*, 2019, **24**, 3918.
20 S. M. Maierean, M. Serban, A. Sahebkar, S. Ursoniu, A. Serban, P. Penson and M. Banach, The effects of cinnamon supplementation on blood lipid concentrations: A systematic review and meta-analysis, *J. Clin. Lipidol.*, 2017, **11**, 1393–1406.
21 J. Zuo, D. Zhao, N. Yu, X. Fang, Q. Mu, Y. Ma, F. Mo, R. Wu, R. Ma, L. Wang, R. Zhu, H. Liu, D. Zhang and S. Gao, Cinnamaldehyde Ameliorates Diet-Induced Obesity in Mice by Inducing Browning of White Adipose Tissue, *Cell. Physiol. Biochem.*, 2017, **42**, 1514–1525.
22 N. Kang, S. Mukherjee and J. Yun, Trans-Cinnamic Acid Stimulates White Fat Browning and Activates Brown Adipocytes, *Nutrients*, 2019, **11**, 577.
23 J. Jiang, Q. Luo, S. Li, T. Tan, K. Xiong, T. Yang and T. Xiao, Cinnamic acid regulates the intestinal microbiome and short-chain fatty acids to treat slow transit constipation, *World J. Gastrointest. Pharmacol. Ther.*, 2023, **14**, 4–21.
24 H. Zhao, H. Wu, M. Duan, R. Liu, Q. Zhu, K. Zhang and L. Wang, Cinnamaldehyde Improves Metabolic Functions in Streptozotocin-Induced Diabetic Mice by Regulating Gut Microbiota, *Drug Des., Dev. Ther.*, 2021, **15**, 2339–2355.
25 J. Kowalska, J. Tyburski, K. Matysiak, M. Jakubowska, J. Łukaszyk and J. Krzymińska, Cinnamon as a Useful Preventive Substance for the Care of Human and Plant Health, *Molecules*, 2021, **26**, 5299.
26 K. Mnafgui, A. Derbali, S. Sayadi, N. Gharsallah, A. Elfeki and N. Allouche, Anti-obesity and cardioprotective effects of cinnamic acid in high fat diet- induced obese rats, *J. Food Sci. Technol. – Mysore*, 2015, **52**, 4369–4377.
27 B. S. Ismail, B. Mahmoud, E. S. Abdel-Reheim, H. A. Soliman, T. M. Ali, B. H. Elesawy and M. Y. Zaky, Cinnamaldehyde Mitigates Atherosclerosis Induced by High-Fat Diet via Modulation of Hyperlipidemia, Oxidative Stress, and Inflammation, *Oxid. Med. Cell. Longevity*, 2022, 4464180.
28 A. Asadi, N. S. Mehr, M. H. Mohamadi, F. Shokri, M. Heidary, N. Sadeghifard and S. Khoshnood, Obesity and

gut-microbiota-brain axis: A narrative review, *J. Clin. Lab. Anal.*, 2022, **36**, e24420.
29 H. Du, L. Shi, Q. Wang, T. Yan, Y. Wang, X. Zhang, C. Yang, Y. Zhao and X. Yang, Fu Brick Tea Polysaccharides Prevent Obesity via Gut Microbiota-Controlled Promotion of Adipocyte Browning and Thermogenesis, *J. Agric. Food Chem.*, 2022, **70**, 13893–13903.
30 Z. Bai, X. Huang, G. Wu, H. Ye, W. Huang, Q. Nie, H. Chen, J. Yin, Y. Chen and S. Nie, Polysaccharides from red kidney bean alleviating hyperglycemia and hyperlipidemia in type 2 diabetic rats via gut microbiota and lipid metabolic modulation, *Food Chem.*, 2023, **404**, 134598.
31 R. Li, X. Yi, J. Yang, Z. Zhu, Y. Wang, X. Liu, X. Huang, Y. Wan, X. Fu, W. Shu, W. Zhang and Z. Wang, Gut Microbiome Signatures in the Progression of Hepatitis B Virus-Induced Liver Disease, *Front. Microbiol.*, 2022, **13**, 916061.
32 H. Zhao, X. Gao, Z. Liu, L. Zhang, X. Fang, J. Sun, Z. Zhang and Y. Sun, Sodium Alginate Prevents Non-Alcoholic Fatty Liver Disease by Modulating the Gut-Liver Axis in High-Fat Diet-Fed Rats, *Nutrients*, 2022, **14**, 4846.
33 N. Larsen, C. B. d. Souza, L. Krych, T. B. Cahú, M. Wiese, W. Kot, K. M. Hansen, A. Blennow, K. Venema and L. Jespersen, *Front. Microbiol.*, 2019, **10**, 223.
34 D. Kang, M. Su, Y. Duan and Y. Huang, Eurotium cristatum, a potential probiotic fungus from Fuzhuan brick tea, alleviated obesity in mice by modulating gut microbiota, *Food Funct.*, 2019, **10**, 5032–5045.
35 Y. Liu, W. Huang, S. Ji, J. Wang, J. Luo and B. Lu, Sophora japonica flowers and their main phytochemical, rutin, regulate chemically induced murine colitis in association with targeting the NF-κB signaling pathway and gut microbiota, *Food Chem.*, 2022, **393**, 133395.
36 M. Yuan, X. Hu, L. Yao, P. Chen, Z. Wang, P. Liu, Z. Xiong, Y. Jiang and L. Li, Causal Relationship Between Gut Microbiota and Liver Cirrhosis: 16S rRNA Sequencing and Mendelian Randomization Analyses, *J. Clin. Transl. Hepatol.*, 2024, **12**, 123–133.
37 X. Liu, B. Mao, J. Gu, J. Wu, S. Cui, G. Wang, J. Zhao, H. Zhang and W. Chen, Blautia-a new functional genus with potential probiotic properties?, *Gut Microbes*, 2021, **13**, 1–21.
38 C. Robert, A. Penhoat, L. Couëdelo, M. Monnoye, D. Rainteau, E. Meugnier, S. Bary, H. Abrous, E. Loizon, P. Krasniqi, S. Chanon, A. Vieille-Marchiset, F. Caillet, S. Danthine, H. Vidal, N. Guillot, P. Gérard, C. Vaysse and M. Michalski, Natural emulsifiers lecithins preserve gut microbiota diversity in relation with specific faecal lipids in high fat-fed mice, *J. Funct. Foods*, 2023, **105**, 105540.
39 X. Jia, W. Xu, L. Zhang, X. Li, R. Wang and S. Wu, Impact of Gut Microbiota and Microbiota-Related Metabolites on Hyperlipidemia, *Front. Cell. Infect. Microbiol.*, 2021, **11**, 634780.
40 A. Papangelis and T. Ulven, Synthesis of Lysophosphatidylcholine and Mixed Phosphatidylcholine, *J. Org. Chem.*, 2022, **87**, 8194–8197.
41 L. Zhang, L. Xiong, L. Fan, H. Diao, M. Tang, E. Luo, W. Guo, X. Yang and S. Xing, Vascular lipidomics analysis reveales increased levels of phosphocholine and lysophosphocholine in atherosclerotic mice, *Nutr. Metab.*, 2023, **20**, 1.
42 C. Zhou, L. Hu, R. Mu, X. Mei, X. Wu, C. Wang and X. Zhou, Compound green tea (CGT) regulates lipid metabolism in high-fat diet induced mice, *RSC Adv.*, 2022, **12**, 24301–24310.
43 G. Chalhoub, A. Jamnik, L. Pajed, S. Kolleritsch, V. Hois, A. Bagaric, D. Prem, A. Tilp, D. Kolb, H. Wolinski, U. Taschler, T. Züllig, G. N. Rechberger, C. Fuchs, M. Trauner, G. Schoiswohl and G. Haemmerle, Carboxylesterase 2a deletion provokes hepatic steatosis and insulin resistance in mice involving impaired diacylglycerol and lysophosphatidylcholine catabolism, *Mol. Metab.*, 2023, **72**, 101725.
44 Z. Yu, N. Wang, D. U. Ahn and M. Ma, Long Term Egg Yolk Consumption Alters Lipid Metabolism and Attenuates Hyperlipidemia in Mice Fed a High-Fat Diet Based on Lipidomics Analysis, *Eur. J. Lipid Sci. Technol.*, 2019, **121**, 1800496.
45 H. Yue, B. Qiu, M. Jia, W. Liu, X. Guo, N. Li, Z. Xu, F. Du, T. Xu and D. Li, Effects of α-linolenic acid intake on blood lipid profiles: a systematic review and meta-analysis of randomized controlled trials, *Crit. Rev. Food Sci. Nutr.*, 2021, **61**, 2894–2910.
46 M. Foucaud-Vignault, Z. Soayfane, C. Ménez, J. Bertrand-Michel, P. G. P. Martin, H. Guillou, X. Collet and A. Lespine, P-glycoprotein dysfunction contributes to hepatic steatosis and obesity in mice, *PLoS One*, 2011, **6**, e23614.
47 D. Miklankova, I. Markova, M. Hüttl, I. Zapletalova, M. Poruba and H. Malinska, Metformin Affects Cardiac Arachidonic Acid Metabolism and Cardiac Lipid Metabolite Storage in a Prediabetic Rat Model, *Int. J. Mol. Sci.*, 2021, **22**, 7680.
48 F. Li, Y. Wang, H. Yu, X. Gao, L. Li, H. Sun and Y. Qin, Arachidonic acid is associated with dyslipidemia and cholesterol-related lipoprotein metabolism signatures, *Front. Cardiovasc. Med.*, 2022, **9**, 1075421.
49 Y. Zhou, H. Khan, J. Xiao and W. Cheang, Effects of Arachidonic Acid Metabolites on Cardiovascular Health and Disease, *Int. J. Mol. Sci.*, 2021, **22**, 12029.
50 K. Tsuge, T. Inazumi, A. Shimamoto and Y. Sugimoto, Molecular mechanisms underlying prostaglandin E2-exacerbated inflammation and immune diseases, *Int. Immunol.*, 2019, **31**, 597–606.
51 F. Sasaki and T. Yokomizo, The leukotriene receptors as therapeutic targets of inflammatory diseases, *Int. Immunol.*, 2019, **31**, 607–615.
52 S. K. Raut and M. Khullar, Oxidative stress in metabolic diseases: current scenario and therapeutic relevance, *Mol. Cell. Biochem.*, 2023, **478**, 185–196.
53 G. Nieto, G. Ros and J. Castillo, Antioxidant and Antimicrobial Properties of Rosemary (Rosmarinus officinalis, L.): A Review, *Medicines*, 2018, **5**, 98.
54 O. Y. Kim and J. Song, Important roles of linoleic acid and α-linolenic acid in regulating cognitive impairment and neuropsychiatric issues in metabolic-related dementia, *Life Sci.*, 2024, **337**, 122356.

